Assessment of low cycle fatigue improvement of machined AISI 316 stainless steel by brush hammering

N. SIDHOM[1], K. MAKHLOUF[1], A. KHLIFI[1], C. BRAHAM[2] and H. SIDHOM[1]

[1]*Laboratoire de Mécanique, Matériaux et Procédés (LR99ES05), ESSTT, University of Tunis, 5 Avenue TahaHusseïn, Montfleury, 1008 Tunis, Tunisia,*

[2]*Laboratoire de Procédés et Ingénierie en Mécanique et Matériaux (PIMM-UMR CNRS 8006), ENSAM, 151, Boulevard de l'Hôpital Cedex 75013, Paris, France*

Received Date: 15 October 2013; Accepted Date: 8 February 2014; Published Online: 24 March 2014

ABSTRACT The effects of wire brush hammering on low cycle fatigue behaviour of AISI 316 austenitic stainless steel has been investigated on turned samples through an experimental study combining strain controlled fatigue tests, scanning electron microscope examination and X-ray diffraction analysis. An increase in fatigue life by 266% was reported at an imposed strain amplitude of $\Delta\varepsilon_t/2 = 0.2\%$. This improvement is limited to $\Delta\varepsilon_t/2 \leq 0.5\%$. It is found that wire brush hammering produces a surface texture that favours, under cyclic loading, nucleation of randomly dispersed short cracks of the order of 50 μm in length stabilized by a compressive residual stress field. In contrast, turned surface showed much longer unstable cracks of the order of 200 μm in length nucleated in the machining groves and propagated under the effect of a tensile residual stress field. It has also been established that wire brush hammering can be used as intermittent treatment to improve the residual fatigue life of components subjected to cyclic loading. The treatment is very efficient if it is performed at a fraction of service lifetime n_i/N_r lower than 0.5.

Keywords fatigue crack; fatigue life; residual stress; stainless steel; wire brush hammering.

NOMENCLATURE

$Hv_{0.05}$ (Hv)	= micro-hardness
n_i/N_r	= fraction of service lifetime
Ra (μm)	= mean roughness
Rt (μm)	= maximum roughness
$\Delta\varepsilon_p$ /2 (%)	= plastic strain amplitude
$\Delta\varepsilon_t$ /2 (%)	= total strain amplitude
σ_0 (MPa)	= residual stress in the loading direction
σ_{90} (MPa)	= residual stress in the transverse direction

INTRODUCTION

Austenitic stainless steels are very important commercial alloys used almost in all industries including automotive, domestic, nuclear, chemical and food processing because of their good resistance to various forms of corrosion combined with satisfactory mechanical properties. These materials also have great aptitude for plastic deformation because of their high ductility. One of the most commonly used grade is AISI 316 stainless steel, which, when used in aerospace and nuclear and chemical industries, revealed other risks of damage in service, including fatigue and corrosion fatigue that depend mainly on the surface topography and on process-induced properties gradient in near surface region.

To improve the surface integrity, mechanical surface treatments such as shot peening,[1–3] ball burnishing,[2,4] deep rolling,[5–7] hammering,[8] laser shock peening[5,9] and brushing[10,11] have been performed on engineering components. These treatments proved to produce significant improvements in terms of fatigue crack initiation and growth resistance as well as stress corrosion cracking resistance. These improvements were largely attributed to induced cold work hardening and compressive residual stress field on surface and in subsurface region.

The shot peening treatment remains the most widely used mechanical surface technique despite its negative effects on the micro-geometric quality of the surface, resulting from the impact of hard particles on the ductile

Correspondence: H. Sidhom. E-mail: habib.sidhom@gmail.com;habib.sidhom@esstt.rnu.tn

material. Such damages have proven to reduce both resistance to localized corrosion, which is one of the main selection criteria of these materials, and the initiation and the first stages of propagation of fatigue cracks due to local micro-stress concentration sites associated to the craters resulting from the treatment. Fathallah *et al.*[1] reported a beneficial effect of shot peening on high cycle fatigue of SAE 3415 caused by compressive residual stress and surface work hardening generated by the treatment in spite of the formation of superficial defects and surface imperfections. This improvement is reported for only a standard 100% coverage, whereas for a severe condition of 1000% coverage, the treatment has become detrimental because of the formation of excessive superficial defects and the micro-geometrical imperfections, which act as stress micro-concentrators favouring surface crack nucleation.

In order to reduce the detrimental effect of excessive surface roughness induced by shot peening, less aggressive techniques were developed. Among these techniques, laser peening,[9] ball and roller burnishing[4] and more recently hammering by wire brush[10–12] were used to replace the shot peening. The efficiency of these techniques has been demonstrated for high cycle fatigue strength of steels and aluminium alloys.[9–11] Laser peening without protective coating applied on SUS304 and SUS316L austenitic stainless steels increased the fatigue strength at 10^8 cycles by a factor of 1.4 and 1.7 compared to the base untreated material in the full heat treated and stress-relieved conditions, respectively.[9] This improvement is attributed by the authors to the conversion of the initial residual stress state near the surface from tensile to a compressive one that reached values up to −1100 MPa for SUS304 and −780 MPa for SUS316L, respectively. This compressive residual stress reached depths as high as 1 mm. Zhang *et al.*[13] showed that roller burnishing is more effective than shot peening in enhancing the fatigue life. Indeed, the roller burnishing, when used at the optimum conditions, improves the high cycle fatigue strength by 110% for AZ80. Concerning wire brushing, Sidhom *et al.*[11] reported that brushing produced compressive residual stresses in the same order as the ones generated by shot peening with the advantage of producing high surface quality to enhance the high cycle fatigue strength by a factor of 20 to 30% for the aluminium alloy AA5083H11. Similarly, Ben Fredj *et al.*[10] investigated the effects of wire brushing on the ground surfaces of AISI 304. They applied three-point bending elastic strain controlled fatigue tests of notched ground samples and found that the brushing operation led to a higher micro-geometrical quality of the surface that increased the endurance limit at 2×10^6 cycles by 26%. This process raised the fatigue strength from 226 to 285 MPa. It appears that this improvement in fatigue decreases rapidly when lower cycles or higher strain fatigue is considered. Moreover, in this high cycle fatigue regime, Ben Fredj *et al*. did not observe a phase transformation induced by fatigue deformation as observed in other cases.[9,14]

The present work aims at proving the numerous technical and economical advantages of the wire brush hammering as an industrial surface mechanical treatment of ductile material parts for plastic fatigue enhancement. Among these advantages are an easy way to implement on-line production, low cost comparative to other surface

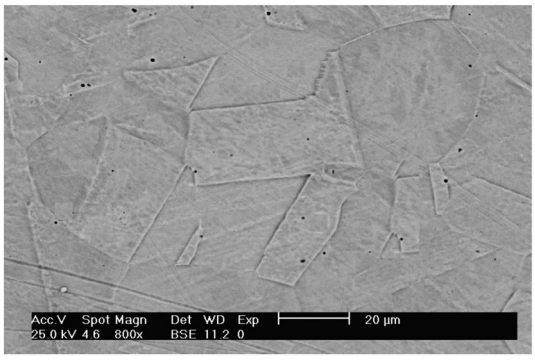

Fig. 1 Structure of the AISI 316 stainless steel.

Table 1 Chemical composition of AISI 316

	Chemical composition (wt%)								
Material	C	Si	Mn	N	Cu	Cr	Ni	Mo	Fe
X5CrNiMo17-12-2 (AISI 316)	0.06	0.05	1.85	0.03	0.05	16.8	12.3	2.59	Balance

Table 2 Mechanical properties of AISI 316

	Tensile mechanical properties					Balk hardness
Material	Yield strength R_e (MPa)	0.2% Offset yield strength $R_{p0.2}$ (MPa)	Tensile strength R_m (MPa)	Young's modulus E (GPa)	Elongation A_r (%)	Hv
AISI 316	266	321	651	196	58	200

treatment processes and the technical possibility to generate a substantial and cyclic stable compressive residual stress without surface damage. The role of surface topography and of surface stabilized compressive residual stresses on the fatigue crack nucleation and growth has been studied by X-ray diffraction and scanning electron microscope (SEM) examination. The beneficial effect of wire brush hammering of AISI 316 on fatigue life has been assessed as an initial and an intermittent surface treatment by strain-controlled fatigue tests. The dependence of this technique on the imposed strain amplitude has also been investigated, and the limiting parameters for the improvement were established.

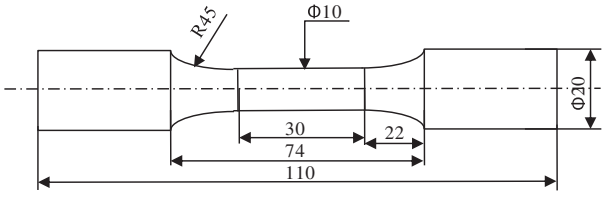

Fig. 2 Fatigue test sample.

MATERIAL AND EXPERIMENTAL PROCEDURES

Material

The material investigated in this study is an AISI 316 austenitic stainless steel. The microstructure of the material is shown in Fig. 1. The chemical composition and the tensile mechanical properties in the solution treated condition are presented in Tables 1 and 2, respectively.

Wire brush hammering

Wire brush hammering was applied to the fatigue samples of the AISI 316 stainless steel, which are obtained by turning (Fig. 2). The cutting parameters for the turning process are given in Table 3. The wire brush hammering operations were conducted on the turned surfaces using stainless steel wire brush as illustrated in Fig. 3. The wire brush characteristics as well as the brushing conditions are given in Table 4. These brushing parameters, which are selected for this study, produce high magnitude and depth of compressive residual

Table 3 Turning conditions of AISI 316

Cutting speed, V_c (m mn^{-1})	Feed rate (mm rev^{-1})	Depth of cut (mm)	Carbide tool beak radius (mm)	Cooling fluid
51	0.05	0.4	0.4	Soluble oil (20%)

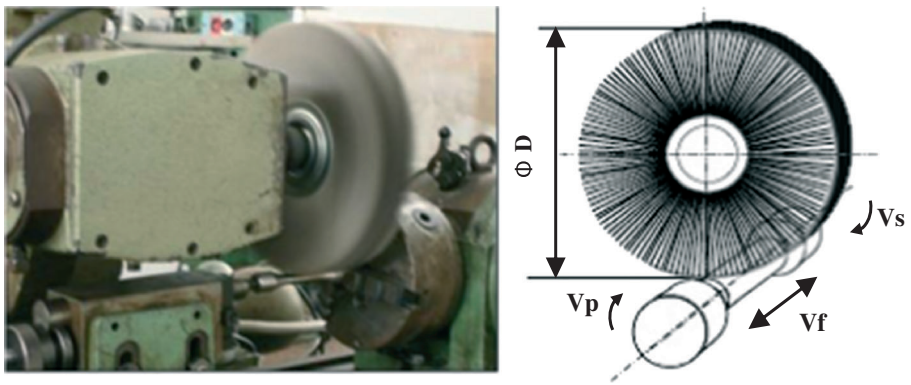

Fig. 3 Wire brush hammering set-up.

Table 4 Wire brush hammering conditions of AISI 316

Brush characteristics		Wire brush hammering conditions	
Brush diameter	$D = 230$ mm	Brush rotation speed	$V_s = 2000$ rpm
Wire diameter	$Ø = 0.1$ mm	Table's feed speed	$V_f = 50$ mm min^{-1}
Wire length	$L = 80$ mm	Number of passes	$N = 10$
Wire material	Stainless steel	Compression percentage[a]	3%

[a]Used length/wire length.

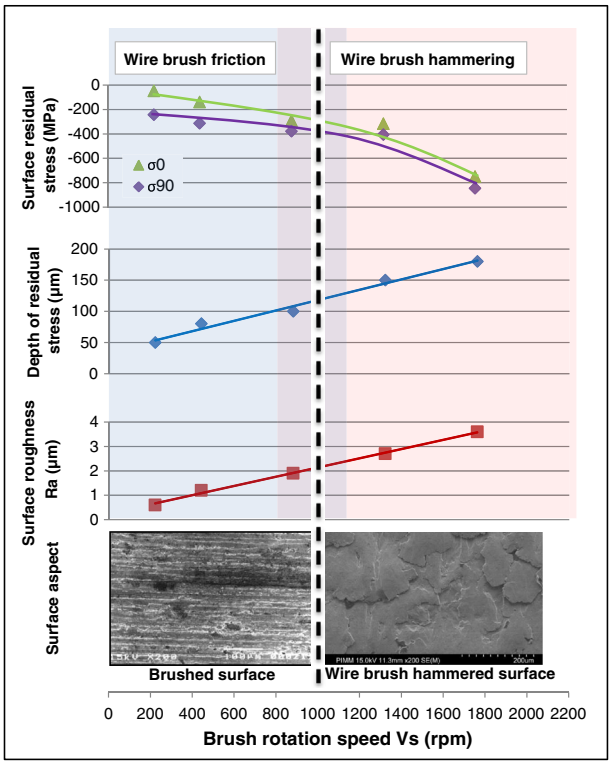

Fig. 4 Effect of brush rotation speed on AISI 316 surface properties ($N = 10$ and $V_f = 50\,\text{mm/mn}^{-1}$).

stresses without significantly increasing the roughness of the surface. These parameters are required for fatigue life improvement. The condition of wire brush hammering is selected on the basis of the result of a study of the effects of brush rotation speed on the near surface aspects and properties of AISI 316 stainless steel. These results are illustrated in Fig. 4. It shows that wire brushing using a brush with the characteristics given in Table 4 leads to a hammered surface similar to that of shot peening for a brush rotation speed higher than 1000 rpm.

Performed tests

Surface characterization tests

Surface hardening induced by turning and wire brush hammering processes and its evolution under cyclic loading was evaluated by micro-hardness ($Hv_{0.05}$) measurements in accordance with ASTM: E384-09. Near surface residual stresses induced by the previously cited processes and their relaxation under cyclic loading were carried out using a Proto LXRD diffractometer (single axis goniometer with Ω geometry). The $\sin^2\Psi$ method was used with the diffraction conditions given in Table 5 in accordance with the NF EN 15305–2009 standard.[15] The in-depth residual stress distribution was determined through iterative electrolytic removal of thin surface layers, using a solution of sulfuric acid (12.5% by volume) and methanol (87.5% by volume).

For initial residual stress distribution, several measurements were carried out in order to verify the homogeneity of the treatment. For stabilized residual stresses, measurements were performed on fatigue samples after failure in a region far enough from the fracture surface (5–10 mm).

Fatigue tests

Tension–compression low cycle fatigue tests ($R_\sigma = -1$) were performed at different total imposed strain amplitudes of $\Delta\varepsilon_t/2 = 0.1$, 0.2, 0.3, 0.5, 0.7 and 1% according to ASTM: E606-04. The frequency was set at 0.1 Hz. The fatigue tests were conducted until fracture of the sample occurred. Hysteresis loops were recorded during the fatigue tests to assess the impact and the improvement limitation of the wire brush hammering operation on the total fatigue life of the sample. In addition, intermittent wire brush hammering operations were carried out on samples at different fractions of the fatigue life to assess the improvement of their residual lifetime.

Fatigue crack examination

Surfaces of unloaded and loaded fatigue specimens as well as fatigue fractured surfaces have been observed using an SEM. Histograms of crack length and depth distributions have been established for quantitative analysis of the role of surface characteristics on the initiation and propagation of fatigue crack resistance.

Table 5 X-ray diffraction conditions for residual stress measurement

Radiation	λ Mn $K_\alpha = 0.2102$ nm
Voltage	20 Kv
Current	5 mA
X-ray diffraction planes	{3 1 1} $2\theta \approx 152°$
Beam diameter	2 mm
Ø angles	0° and 90°
Ψ oscillation	±3°
Ψ angles	−37.27 −33.21 −28.88 −24.09 −18.43 −10.52 0.00 14.96 21.42 26.57 31.09 35.26 39.23

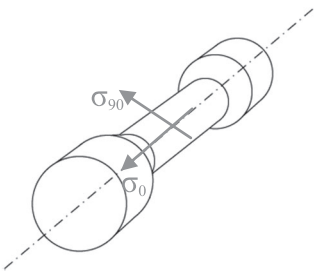

Table 6 Characteristics of turned and brush-hammered surfaces of AISI 316

	A		B			C		D
	Roughness, µm		Micro-hardness, $Hv_{0.05}$			Near surface residual stress level, MPa		Surface texture
Finishing mode	R_a	R_t	Near surface $(Hv)_s$	Bulk material $(Hv)_b$	Cold work hardened thickness (µm)	Loading direction (σ_0)	Transversal direction (σ_{90})	
Turning	2.31	10.02	330	200	160	$-14^{\pm 30}$	$340^{\pm 30}$	Machining grooves
Turning + brushing	3.65	15.26	440	200	180	$-846^{\pm 24}$	$-750^{\pm 32}$	Overlaps

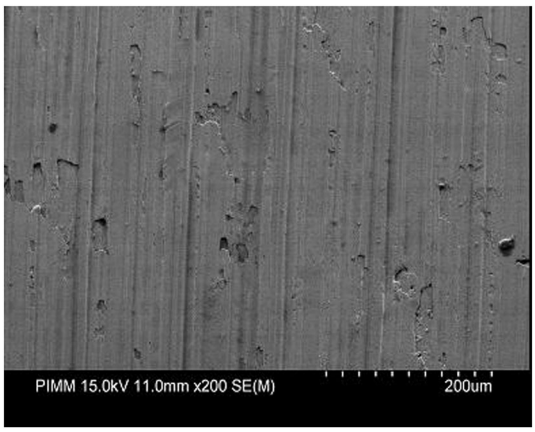

Fig. 5 Surface texture of turned AISI 316 stainless steel.

RESULTS

Surface quality evaluation

The different surface characteristics for the turned and wire brush-hammered samples are summarized in Table 6.

Surface aspects and roughness

The surface topography is characterized by mean (R_a) and maximum (R_t) roughness values as indicated in column A of Table 6. The SEM examination reveals that the surface texture for the turned samples is marked by grooves as illustrated in Fig. 5, whereas wire brush-hammered samples present an aspect of blasted surface as a result of successive strikes of the steel wires of the brush on the surface. These features are shown in Fig. 6.

Near surface cold work hardening

The plastic-induced cold work hardening was described by micro-hardness profiles ($Hv_{0.05}$) as seen in Fig. 7. A stronger hardening gradient for the wire brush-hammered surface compared to the machined surface is

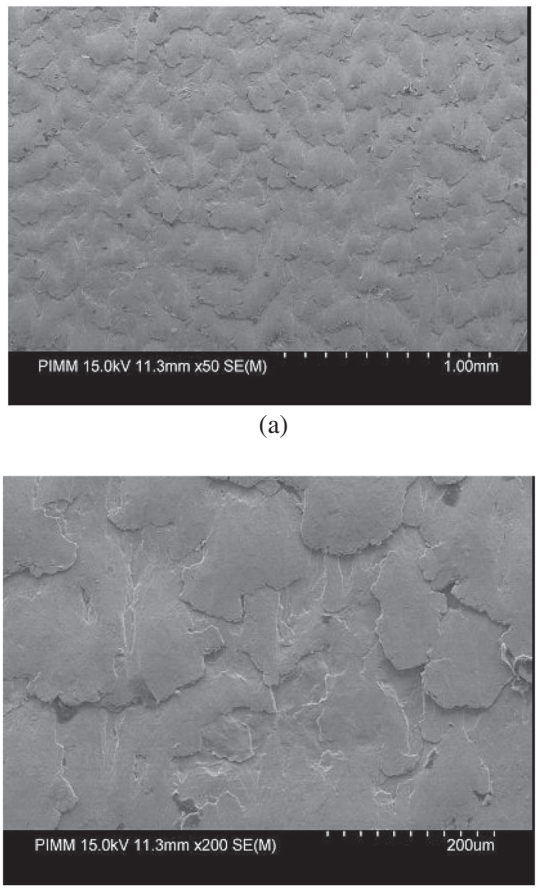

Fig. 6 Surface texture of wire brush-hammered AISI 316 stainless steel: (a) general aspect and (b) overlaps produced by the treatment.

clearly observed. A surface hardness of 440 Hv is measured for the wire brush-hammered material, whereas only a value of 330 Hv is measured for the machined surface. These values are compared to the bulk hardness of the material, which is equal to 200 Hv. Therefore, the rate of the hardening of the surface with respect to the bulk material is increased by 120 and 65 % for the wire brush-hammered and for the turned surfaces, respectively, as

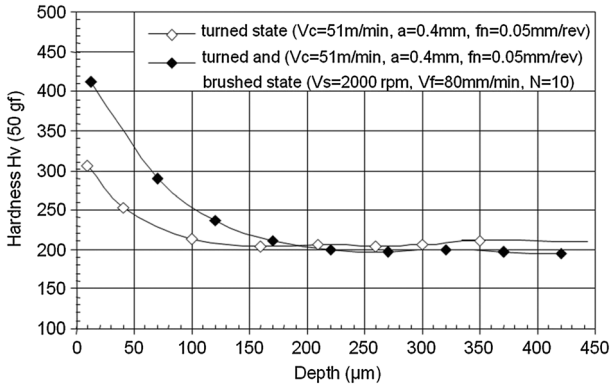

Fig. 7 Surface cold work hardening resulting from turning and wire brush hammering of AISI 316 stainless steel surfaces.

shown in column B of Table 6. The extent of the cold work hardening is comparable for both surface preparation modes (turned and brush-hammered), and it reached approximately 200 µm underneath the surface.

Near surface residual stress

Machining and wire brush-hammering operations induce residual stresses in the processing-affected layers. In the case of wire brush hammering, the residual stresses are generated by wire brush bombarding of the surface leading to plastic deformation of thin surface layers. The plastic deformation changes the dislocation density and the inter-planar spacing of the crystal lattice, which is evaluated by X-ray diffraction. The elastic subsurface layers should theoretically recover to their original shape during unloading. However, continuity conditions between the elastic and plastic zones do not allow for this to occur. Consequently, a compressive residual stress field is developed in the near surface layer while tensile residual stresses are present underneath the layer. Globally, the residual stress field is self-equilibrated as illustrated by residual stress profile (Fig. 8). The profile of turning-induced residual stress is compared to that of the hammering-induced one in Fig. 8. The near surface residual stress levels are reported in column C of Table 6. It shows that turning induces tensile residual stress ($\sigma_{90} = 340$ MPa) in the transversal direction, which is converted to a compressive one ($\sigma_{90} = -750$ MPa) by the wire brush-hammering operation. This last has a value higher than the yield and ultimate strength of bulk material but certainly below those of the highly deformed layers. Indeed, the excessive bombardment of the surface by the wire brush induces a significant work hardening (i.e. an increase of the yield strength) in the near surface layers as illustrated by the hardness profile (Fig. 7) and consequently the mechanical properties, which are related to the treatment-induced deformation substructure in the upper layer. For this material (AISI 316), higher

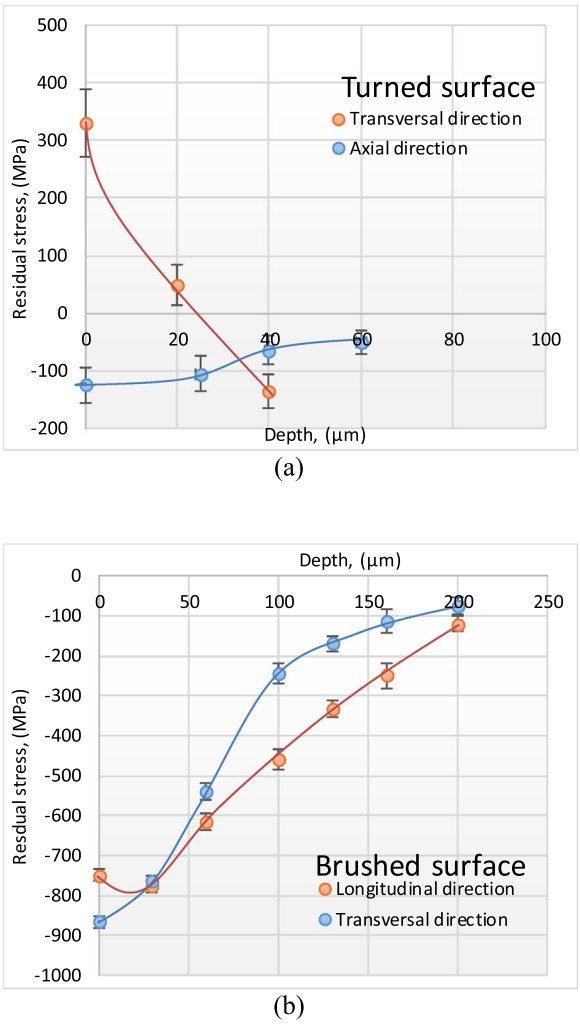

Fig. 8 Near surface residual stress distribution: (a) the turned sample and (b) wire brush-hammered sample.

tensile residual stress (above 1000 MPa) has been reported by Moussa *et al.*[16] after turning in orthogonal cutting conditions. Residual stress profiles originated by processing-induced plasticity could well be correlated with the hardness profiles given in Fig. 7. These profiles show a deep affected layer by the brushing operation (150–200 µm) compared to the turning process (50–100 µm). The brushing-induced residual stresses are almost the same for both axial and transversal directions. The values of the surface brushed residual stresses are relatively comparable to those usually generated by shot peening treatment whereas the depth of the affected layer is lower.

Fatigue life evaluation

Fatigue lifetime results of the initial and intermittent wire brush hammering are compared to those of the turned state in order to evaluate the rate of improvement resulting from these treatments.

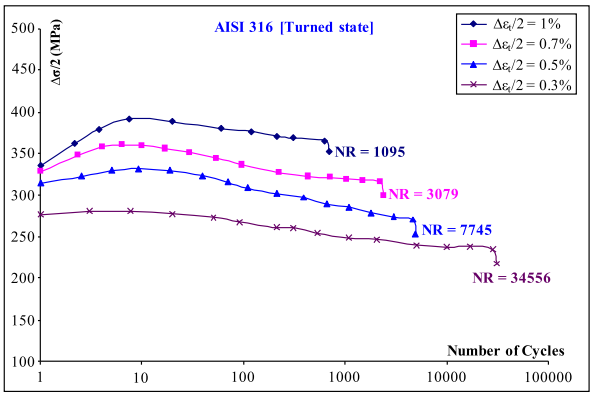

(a)

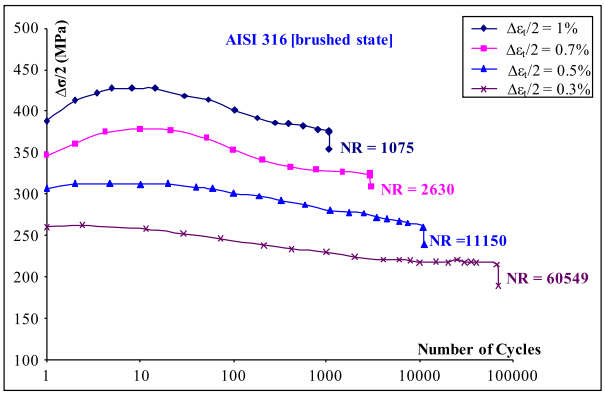

(b)

Fig. 9 Cyclic stress versus number of cycles curves at different strain amplitudes for (a) turned samples and (b) wire brush-hammered samples.

Effect of initial wire brush hammering

Cyclic stress versus number of cycles curves of wire brush-hammered surfaces show a strengthening followed by a softening phase before fracture for all imposed strain amplitudes (Fig. 9a & b). It is important to notice that cyclic strengthening is more important as the strain amplitude is higher.

Results of fatigue life reported in Table 7 show a considerable gain in terms of the number of cycles to failure resulting from wire brush hammering treatment compared to turning, which is considered as a reference state. Indeed, the fatigue lifetime at $\Delta\varepsilon_t/2 = 0.2\%$ for the wire brush-hammered sample is found to be 266% higher with respect to the turned sate. However, this increase of fatigue lifetime is reduced as the strain amplitude is increased. Therefore, the efficiency of wire brush hammering is shown to be limited to total strain amplitudes $\Delta\varepsilon_t/2 = 0.5\%$. On the contrary, the beneficial effect of the mechanical brush hammering after machining is completely cancelled or even reversed when the imposed strain amplitude becomes more important. Indeed, for the imposed strain amplitudes of $\Delta\varepsilon_t/2 = 0.7\%$ or 1%, the fatigue lifetime of wire brush-hammered samples is slightly lower than that of the turned samples. Consequently, 0.5% total imposed strain amplitude could be considered as the upper limit parameter for fatigue life improvement by wire brush hammering of AISI 316 stainless steel.

Effect of intermittent wire brush hammering

The efficiency of intermittent wire brush hammering as an onsite residual service lifetime improvement method of AISI 316 components subjected to low cyclic plastic deformation has also been assessed. Therefore, intermittent wire brush hammering treatments have been performed on the turned surface at various lifetime fractions $n_i/N_r = 0.16$, 0.25 and 0.5 and at various strain amplitudes of $\Delta\varepsilon_t/2 = 0.2$, 0.3 and 0.5%. The efficiency of the intermittent wire brush hammering is evaluated

Table 7 Fatigue lifetime improvement by mechanical wire brush hammering of AISI 316

	Low cycles fatigue test conditions				Number of cycles to fracture N_R		
					Surface finishing mode		
Material	Test temperature Θ (°C)	Frequency (Hz)	Load ratio	$\frac{\Delta\varepsilon_t}{2}$ (%)	Turning	Turning + brushing	Improvement rate (%)
AISI 316	$T = 20$	$f = 0.1$	$R = -1$	0.1	Not fractured	Not fractured	—
				0.2	**109 876** (109 876; 111 450)	**402 697** (402 687; 414 340)	**266**
				0.3	**34 556** (34 556; 35 790)	**60 549** (60 549; 60 938)	**75**
				0.5	**7745** (7745; 8370)	**11 150** (11 150; 11 351)	**44**
				0.7	**3079** (3079; 3178)	**2630** (2630, 2960)	Detrimental effect
				1	**1095** (1095; 1190)	**1075** (1075; 1110)	Detrimental effect

Bold numbers represent the most conservative fatigue test results. Numbers between parentheses represent results of two fatigue tests under the same conditions.

[a]Improvement rate with respect to turned surface.

Table 8 Assessment of the effects of intermittent brushing on the remaining fatigue life of components manufactured from AISI 316 and subjected to cyclic loading

Imposed strain amplitude $\frac{\Delta\varepsilon_t}{2}$ (%)	Lifetime of component after turning N_R (cycle)	Fraction of lifetime in service n_i/N_R	Total lifetime of brushed component N_R (cycle)	Improvement rate of residual lifetime, $\Delta N/N$ (%)
0.2	109 876	0	402 697	266
		0.16	286 453	160
		0.25	161 583	47
		0.5	116 980	6
0.3	34556	0	60 549	76
		0.16	50 450	59
		0.25	43 587	34
		0.5	38 550	12
0.5	7745	0	11 150	44
		0.16	9870	32
		0.25	9035	22
		0.5	8150	10

experimentally by the rate of residual fatigue lifetime increase. The results summarized in Table 8 show that intermittent brush hammering remains an efficient surface treatment to extend the residual service lifetime of AISI 316 components loaded at imposed strain amplitudes $\Delta\varepsilon_t/2 \leq 0.5\%$. Moreover, the intermittent treatment is more beneficial when it is performed at low n_i/N_r values. In all cases, brushing performed at n_i/N_r higher than 0.5 is considered to be an inefficient improvement operation. Nevertheless, a significant improvement in the residual lifetime at $\Delta\varepsilon_t/2 = 0.2\%$, ranging from 160 to 6% is reported when the brushing operation is applied on the surface sample at $n_i/N_r = 0.16$ and $n_i/N_r = 0.5$ of the total life of the component, respectively. For strain amplitudes of $\Delta\varepsilon_t/2$ of 0.3 and 0.5%, the improvements of the residual life are less significant. They range between 59 and 10%.

Effects of surface characteristics on the fatigue crack nucleation and growth

The fatigue life improvements reported for the initial and intermittent wire brush hammering are likely to be controlled by the effects of residual stress, by cold work hardening and by surface texture on the fatigue crack nucleation and growth.

Effects of stabilized residual stress and cold work hardening on fatigue crack nucleation

The initial residual stress distribution induced by turning or wire brush hammering could be altered under cyclic loading. Therefore, the near surface stabilized residual stress values have been determined by X-ray measurements performed on the fatigue samples away from the fractured surface. The results summarized in Table 9 show no or a slight relaxation of the near surface residual stress at low imposed strain amplitudes ($\Delta\varepsilon_t/2 = 0.5\%$) for both machined and wire brush-hammered treatments. However, for high strain amplitudes, the stabilized residual stress of turned surface undergoes an important relaxation (transversal direction) or shifts gradually to compressive value because of higher cyclic plastic deformation (loading direction). As for the brush-hammered surface, the same phenomenon seems to occur. The high stability of brush hammering compressive residual stress is due to the effect of high and deep cold work hardening

Table 9 Cyclic stabilized near surface residual stresses of AISI 316 turned and wire brush hammered

Imposed strain amplitude $\Delta\varepsilon_t/2$ (%)	Surface preparation mode			
	Turned surface residual stress		Brushed surface residual stress	
	Loading direction	Transverse direction	Loading direction	Transverse direction
Unloaded	−14 ± 30	340 ± 30	−846 ± 24	−750 ± 32
0.1	N.R.	N.R.	−903 ± 16	−736 ± 40
0.2	N.R.	N.R.	−870 ± 15	−700 ± 20
0.3	−179 ± 22	118 ± 20	−490 ± 13	−136 ± 24
0.5	−312 ± 34	217 ± 52	−813 ± 12	−477 ± 20
0.7	−511 ± 38	335 ± 28	−197 ± 9	132 ± 7
1	−265 ± 16	55 ± 18	−640 ± 17	−353 ± 12

N.R., no significant relaxation observed.

induced by this process compared to machined one as illustrated in Fig. 6. Then, the beneficial effects of the brushing induced compressive residual stresses, and cold work hardening on the fatigue crack nucleation strength is maintained for imposed strain amplitudes lower than 0.5% as it is confirmed by the fatigue life enhancement reported in Table 7. The major fraction of residual stress relaxation occurs, as reported by several authors,[17,18] during the first loading cycle as an effect of static loading resulting from loading at levels exceeding the material yielding, which produces a change of plastic misfit between surface layer and bulk material. Then, the relaxation does not occur when the total (applied and residual stress) is below the material yield stress. During cycling, the relaxation gradually increases depending on material behaviour, loading conditions and number of cycles. It is also reported that the greater the applied tension or imposed strain, the greater the relaxation of the residual stress.[19,20] This phenomenon has been globally observed in this study for both machined and wire brushed conditions although the quantitative comparison with literature data is not possible because of the difference of materials and loading conditions.

Effects of surface texture on the distribution of fatigue crack nucleation sites

SEM analysis of the fatigue sample surfaces revealed different distributions of fatigue crack initiation sites for each surface preparation mode.

(a) Turned surface: cyclic loading produces short micro-cracks of 50–200 μm in length initiating exclusively in the machining grooves as shown in Fig. 10a. These grooves act as preferential sites for fatigue crack nucleation because they represent local stress concentration zones. Interaction between the stress fields at the tip of each micro-crack will cause coalescence across the narrow grooves (Fig. 10b). The coalescence produces longer fatigue crack of few millimetres in length encircling the sample and perpendicular to the loading direction (Fig. 10c). One of these long cracks leads eventually to propagation in depth until fracture of the sample.

(b) Wire brushed surface: in this case, short fatigue micro-cracks of length between 20 and 50 microns (arrows) are randomly distributed with no evident dependence on the surface texture (Fig. 11a). Therefore, the coalescence is delayed with respect to the turned case characterized by fatigue micro-cracks localized inside the narrow grooves. These cracks will also coalesce after a greater number of loading cycles and produce long fatigue cracks of the order of 100–500 μm in length (Fig. 11b).

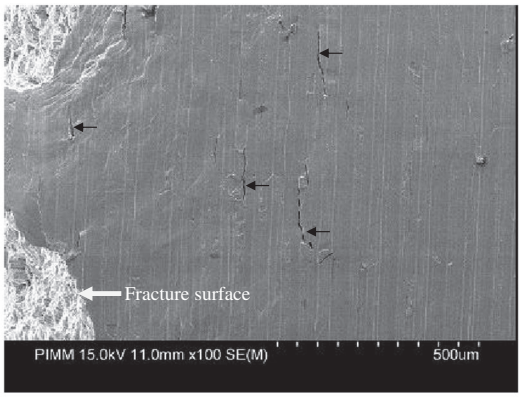

(a)

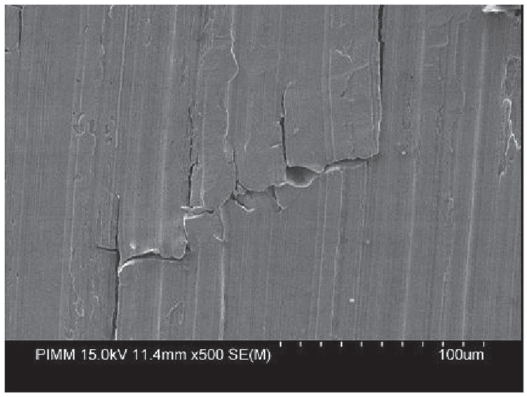

(b)

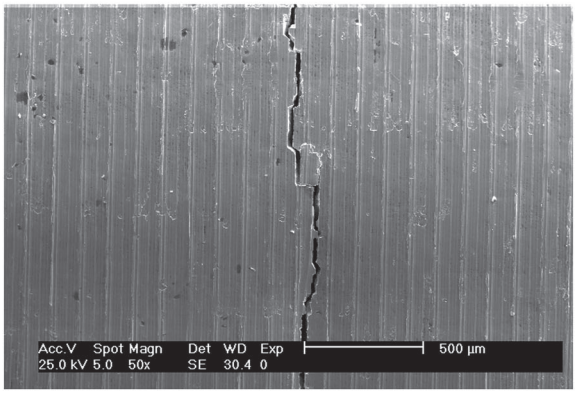

(c)

Fig. 10 SEM micrographs of turned surface fatigue sample showing fatigue cracks nucleation sites: (a) short micro-cracks initiating inside the machining grooves, (b) coalescence of the surface short micro-cracks and (c) longer fatigue cracks resulting from coalescence of micro-cracks. The fatigue test was performed at $\Delta\varepsilon_t/2 = 0.3\%$.

Eventually, one of these cracks will produce the final fracture. These cracks are presumed to be more stable with respect to coalescence and propagation under the effects of the brushing-induced compressive residual stress field (−490 MPa). This stress field impedes considerably their growth and coalescence

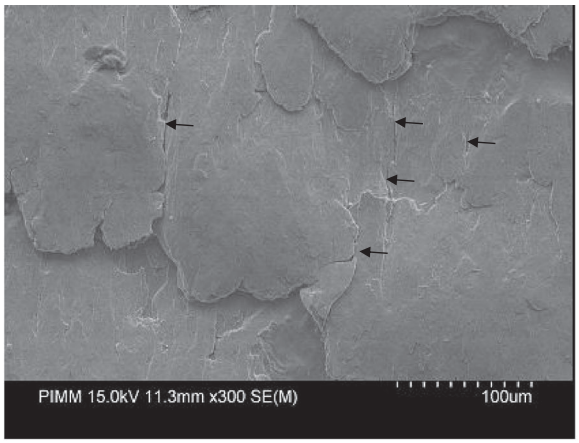

(a)

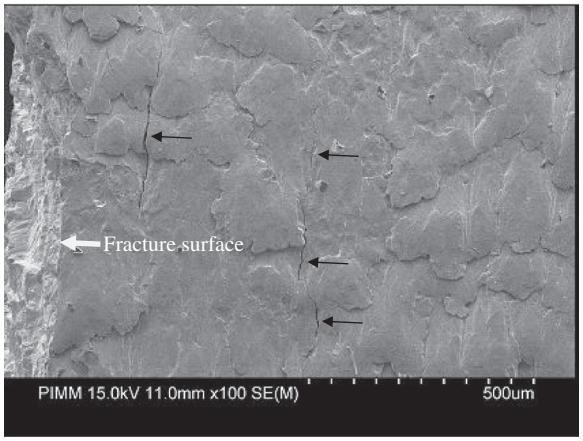

(b)

Fig. 11 SEM micrographs of wire brush-hammered surface fatigue sample showing fatigue cracks nucleation sites: (a) rare short micro-cracks randomly distributed and (b) longer fatigue cracks resulting from short micro-cracks coalescence. The fatigue test was performed at $\Delta\varepsilon_t/2 = 0.3\%$.

even after partial cyclic relaxation, as observed in Table 9. These observations explain well the fatigue life improvement produced by the brush hammering operation (60 529 cycles) compared to the turning process (34 556 cycles) of samples loaded under the same conditions ($\Delta\varepsilon_t/2 = 0.3\%$).

Effects of cold work hardening and residual stress on fatigue crack propagation

Propagation of surface-nucleated fatigue cracks has been evaluated by the statistical distribution of the depth in cross-sectional cuts of the fatigue samples and by surface fracture characteristics of both turned and wire brush-hammered surfaces:

(a) Depth of fatigue cracks

SEM analysis of cross-sectional cuts of the fatigue samples tested at $\Delta\varepsilon_t/2 = 0.3\%$ revealed a different depth distribution of the surface-nucleated fatigue cracks depending on the surface preparation mode (Fig. 11). It has been observed that surface-nucleated fatigue cracks propagate more rapidly for the turned case than for the wire brush-hammered one. Indeed, a qualitative examination of cross sections of the samples revealed a multitude of short cracks of the order of 50 μm in length, whereas more and shorter cracks are seen on the wire brush-hammered surface as illustrated in Fig. 12a and b. A histogram of crack density as a function of crack depth indicates that the fraction of damaging cracks ($l \geq 200$ μm) is greater for the turned surface than for the wire bush hammered one (Fig. 13). This distribution in fatigue micro-cracks depth is consistent with surface fatigue crack distribution as illustrated in SEM micrograph taken at high magnification (Fig. 14). Then, it is demonstrated that wire brush-hammered surface

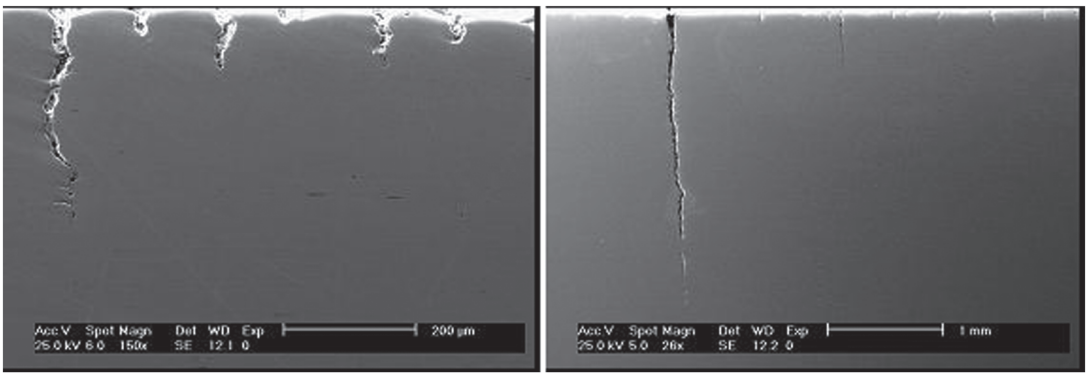

(a) (b)

Fig. 12 Fatigue cracks depth distribution: (a) turned surface and (b) wire brush-hammered surface. The fatigue test was performed at $\Delta\varepsilon_t/2 = 0.3\%$.

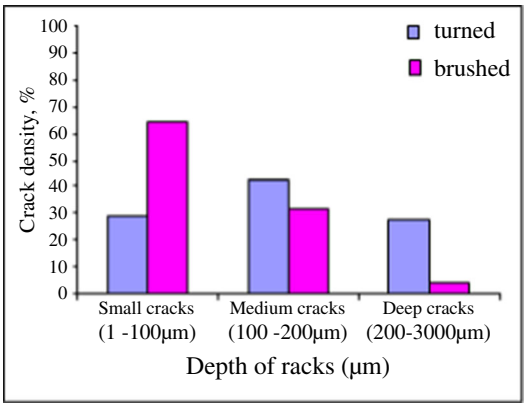

Fig. 13 Histogram of fatigue crack density as a function of crack size for turned and brushed surfaces. The fatigue test was performed at $\Delta\varepsilon_t/2 = 0.3\%$.

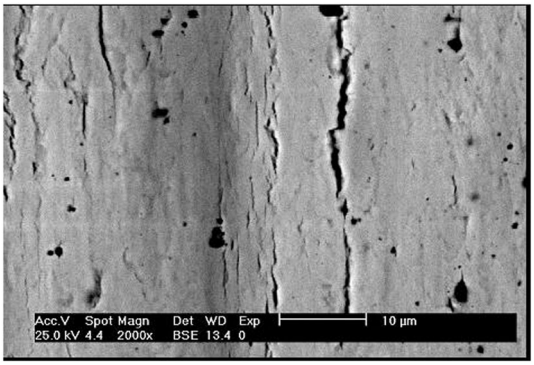

Fig. 14 Short and small micro-cracks distribution on the wire brush-hammered surface after loading at $\Delta\varepsilon_t/2 = 0.3\%$ until fracture (high magnification).

presents a better resistance in terms of crack propagation than the turned surface. This behaviour could be attributed to the beneficial effect of the stabilized compressive residual stresses induced by the wire brush hammering operation on the propagation of the initiated cracks.

(b) Fracture surface

SEM fatigue fracture surfaces indicate that crack initiation is produced on the surface of the sample for both surface preparation modes as seen in Fig. 15a. However, the propagation from these initiation sites occurs in a brittle manner through the hardened layer produced by turning or wire brush hammering operations as seen in Fig. 15b. This hardened layer is of the order of 200 μm as expected from the hardness profiles given in Fig. 6. After this hardened layer, the fatigue cracks propagate in a ductile manner producing the classical fatigue striations as seen in Fig. 15c. Then, it is demonstrated that cold work hardening, which is higher and deeper for wire brush hammering process, is detrimental for the propagation stage.

DISCUSSION

The results of this study complete the already existing data on the relative improvement of high cycle fatigue crack resistance of different materials by surface brushing treatments.[10,11,21] In fact, it is established in this study that the beneficial effects of wire brush hammering could be extended to the low cycle fatigue regime of AISI 316 stainless steel. For this steel, fatigue life improvement equal to 266% was reported for a total strain amplitude $\Delta\varepsilon_t/2 = 0.2\%$. This value is slightly lower than that reported for AISI 304 stainless steel, which reached a value of 307% at the same total imposed strain amplitude.[12] However, the improvement is limited to total deformation rates $\Delta\varepsilon_t/2 \leq 0.5\%$ (corresponding to a plastic strain amplitude $\Delta\varepsilon_p/2 \leq 0.347\%$) as shown in Table 7. In addition, it is also shown in this study that the beneficial effects of wire brush hammering in terms of prolonging the residual lifetime of components can be extended to be applied on site as an intermitted treatment. The efficiency of this intermittent treatment is more significant for strain amplitudes lower than 0.5% and only if performed in the early stages of the component service lifetime. It is found that this intermittent treatment increases the service lifetime of the sample by 160% when applied at $n_i/N_r = 0.16$. The efficiency of wire brush hammering as post-machining treatment resides in increasing the fatigue crack initiation and propagation resistance of surface layers, which are controlled by surface texture and stabilized near surface properties. It is shown through an investigation of surface characteristics related to crack initiation and propagation mechanisms that the wire brush hammering acts favourably in modifying the potential crack initiation sites, the residual stress state and the surface hardening phenomena. The combined effects of these three phenomena explain the low cycle fatigue life improvement of AISI 316 stainless steel when subjected to wire brush hammering as initial or intermittent treatments.

Efficiency of initial wire brush hammering

SEM examination of the fatigue crack networks and fatigue fracture surface coupled with X-ray residual stress measurement prove that the experimentally assessed fatigue life improvements are the result of the beneficial effects of the treated surface such as surface texture, surface hardening and stabilized compressive residual stress.

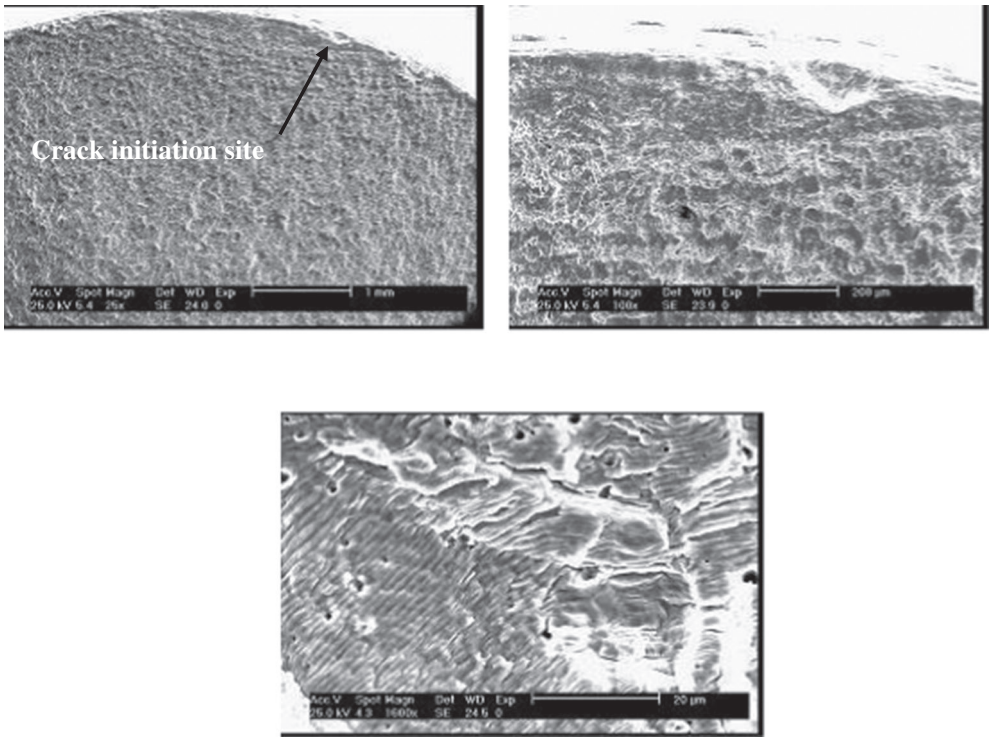

Fig. 15 Fatigue fracture of wire brush-hammered surface: (a) initiation site at the surface, (b) brittle propagation in the hardened layer and (c) ductile fatigue striations outside the hardened layer. The fatigue test was performed at $\Delta\varepsilon_t/2 = 0.3\%$.

Contribution of surface texture

Unlike shot peening,[1,22,23] hammering by steel wire brush of the ductile AISI 316 stainless steel does not alter significantly the surface roughness and does not induce large defects as in the case of ductile material AISI 304 stainless steel[10,12] and AA 5083.[11] It is found that the arithmetic average surface roughness, R_a, increased slightly from 2.31 to 3.65 μm as a result of wire brush hammering whereas the maximum surface roughness, R_t, increased significantly from 10.02 to 15.26 μm. These results are different from those generated by Ben Fredj *et al.*[10] on ground surfaces of AISI 304 stainless steel where they reported a decrease in R_t values by 60% and no change in R_a when the surface has received a wire brushing treatment. In addition, like shot peening, wire brush hammering treatment seems to reduce or eliminate the surface grooves produced during machining operation. These surface grooves obviously represent preferential sites for micro-stress concentration. Therefore, wire brush hammering modifies the surface texture and gives the material a specific topography such as overlaps as a result of the impact of the steel wires of the brush on the surface. These features, with much less depth than those of the grooves, regularly cover the surface of the sample. This phenomenon led to the formation of short fatigue crack networks that retard the crack propagation and coalescence under cyclic loading. This explains partially the improvement produced by the wire brush hammering treatment as evidenced by comparing Figs 10 and 11.

Contribution of surface cold work hardening

The turning process induces cold work hardening (330 Hv) of the sample surface comparative to the bulk material (200 Hv), whereas subsequent wire brush hammering produces much harder surface that reached a hardness of 440 Hv. The depth of the hardened layer is around 200 μm. This high surface hardness is expected to contribute significantly to the enhancement of fatigue crack initiation resistance near surface as reported in previous studies.[10,12] Ben Fredj *et al.*[10] reported a 26% increase in the high cycle fatigue strength of a ground and brushed AISI 304 stainless steel sample, whereas Makhlouf *et al.*[12] reported an increase in low cycle fatigue life by 307% at a strain amplitude $\Delta\varepsilon_t/2 = 0.2\%$ for a turned AISI 304 stainless steel. This last value is of the same order of magnitude (266%) found in this study for AISI 316. It is clear that the induced hardened layer increases the nucleation stage resistance, whereas it accelerates the first stage of fatigue crack propagation as illustrated by SEM fractographs given in Fig. 15 showing the brittle aspect of the hardened layer fracture.

Contribution of residual stress

It is well established that residual stresses have a significant effect on nucleation and growth of fatigue cracks during cyclic loading. The machining-induced tensile residual stress exhibits a detrimental effect by promoting long crack initiation (Fig. 10) and rapid propagation ($da/dN = C(\Delta K_{eff})^n$) resulting from high effective stress intensity (K_{eff}), which is the sum ($K_{eff} = K_S + K_{RES}$) of the stress intensity due to external loading (K_S) and the stress intensity due to the tensile residual stress (K_{RES}). On the other hand, the hammering-induced compressive residual stress near the surface caused shallow cracks (Fig. 11) that tend to propagate slowly than observed for machined case with tensile residual stress. In this case, the effective stress intensity is reduced by the negative residual stress intensity factor. These observations are in good agreement with both experimental and modelling results reported in the literature for both ductile and hard materials.[1,10–12,20,25] Indeed, the turning process produces tensile or very low compressive residual stresses in both loading and transverse directions ($\sigma_0 = -14$ MPa in the loading direction and $\sigma_{90} = +340$ MPa in the transverse direction), whereas subsequent wire brush hammering operation reverses those residual stresses to induce highly compressive ones ($\sigma_0 = -846$ MPa and $\sigma_{90} = -750$ MPa in the same directions, respectively). Still, these residual stresses relax significantly when the sample undergoes imposed cyclic strain loadings at higher strain amplitudes as seen in Table 9. The stabilized values remain compressive and therefore beneficial for fatigue crack nucleation and growth resistance. That is why the efficiency of wire brush hammering is more significant when the imposed plastic strain amplitude is low ($\Delta\varepsilon_t/2 \leq 0.2\%$) favouring high stabilized compressive residual stress.

It is obvious that wire brush-hammered surface has an advantageous texture in which fatigue crack nucleation networks are more stabilized by the compressive residual stress field leading to a higher fatigue life comparative to the turned surface. For the turned surface, unstable long cracks coalesce and propagate rapidly in a tensile or low plastic cyclic induced compressive residual stress field. As the strain amplitude is increased, the beneficial effects of the wire brush hammering operation are reduced as a result of cyclic stress relaxation as shown in Table 9. These results are in good agreement with those obtained for shot-peened surfaces of ductile material[22–24] and brushed surface of AISI 304[12] and aluminium alloys[11,21]

Fatigue life improvement resulting from intermittent brushing operation

It is shown in this study that intermittent brushing that could be carried out on site on AISI 316 stainless steel components can indeed improve the residual fatigue lifetime of those components. However, this improvement can be achieved for strain amplitudes lower than 0.5% and when the treatment is performed early in the service lifetime characterized by n_i/N_r lower than 0.5. As it is reported in Table 8, at a $n_i/N_r = 0.25$, the improvement rate of the residual lifetime is reduced from 47% at a strain amplitude $\Delta\varepsilon_t/2 = 0.2$–22% at a strain amplitude $\Delta\varepsilon_t/2 = 0.5\%$. These improvements are comparable (53 and 24%, respectively) to those obtained for AISI 304 stainless steel under the same loading condition ($\Delta\varepsilon_t/2 = 0.2$ and 0.5%) and for the same surface preparation mode (turning and wire brush hammering).[12] This improvement is, as discussed previously, the result of the enhancement of the surface texture, surface cold work hardening and compressive residual stresses induced by the wire brush hammering operation. In addition, it is also reported that this improvement depends on strain amplitude. As the strain amplitude is increased, the improvement is reduced or annihilated.

CONCLUSIONS

Based on the investigation of the effects of the wire brush hammering operation as a method to improve service fatigue life of machined components in AISI 316 stainless steel, the following conclusions can be made:

- Surface changes

Wire brush hammering operation did not alter significantly the surface topography in terms of roughness, but it reduced significantly the surface grooves produced during the turning operation. It also increased significantly the surface hardness from around 200 to 440 Hv. The depth of the hardened layer is around 200 μm. Moreover, this post-machining treatment shifts the tensile surface residual stress field (340 MPa) in the machined state to a compressive one (−750 to −840 MPa) in the brushed state. These residual stresses remain stable for imposed cyclic strain amplitudes $\Delta\varepsilon_t/2 \leq 0.5\%$.

- Low cycle fatigue life improvement

An increase in fatigue lifetime by over 266% has been achieved for low strain amplitude of $\Delta\varepsilon_t/2 = 0.2\%$ by initial wire brush hammering. The improvement is limited to strain amplitudes $\Delta\varepsilon_t/2 \leq 0.5\%$. The intermittent wire brush hammering was found to be beneficial if performed in the early stages of the component service lifetime ($n_i/N_r \leq 0.3$) and for strain amplitudes lower than 0.5%. These improvements are the result of the combined contribution of surface texture, strain hardening and stabilized compressive residual stress on the fatigue crack nucleation and growth resistance.

REFERENCES

1 Fathallah, R., Laamouri, A., Sidhom, H. and Braham, C. (2004) High cycle fatigue behavior prediction of shot-peened parts. *Int. J. Fatig.*, **26**, 1053–1067.

2 Mhaede, M. (2012) Influence of surface treatments on surface layer properties, fatigue and corrosion fatigue performance of AA7075 T7. *Mater. Des.*, **41**, 61–66.

3 Azar, V., Hashemi, B. and Yazdi, M. R. (2010) The effects of shot peening on fatigue and corrosion behavior of 316 L stainless steel in Ringer's solution. *Surf. Coating. Tech.*, **204**, 3546–3551.

4 Hassan, A. M. (1997) The effects of ball and roller burnishing on the surface roughness and hardness of some non-ferrous metals. *J. Mater. Process. Technol.*, **72**, 385–391.

5 Nikitin, I., Scholtes, B., Maier, H. J. and Altenberger, I. (2004) High temperature fatigue behavior and residual stress stability of laser-shock peened and deep rolled austenitic steel AISI 304. *ScriptaMaterialia*, **50**, 1345–1350.

6 Nikitin, I. and Besel, M. (2008) Correlation between residual stress and plastic strain amplitude during low cycle fatigue of mechanically surface treated austenitic stainless steel AISI 304 and ferritic-perlitic steel SAE 1045. *Mater. Sci. Eng. A*, **491**, 297–303.

7 Brinksmeier, E., Garbrecht, M. and Meyer, D. (2008) Cold surface hardening. *CIRP Ann. Manuf. Technol.*, **57**, 541–544.

8 Hacini, L., Van Lê, N. and Bocher, P. (2008) Effects of impact energy on residual stresses induced by hammer peening of 304L plates. *J. Mater. Process. Technol.*, **208**, 542–548.

9 Sano, Y., Obata, M., Kubo, T., Mukai, N., Yoda, M., Masaki, K. and Ochi, Y. (2006) Retardation of crack initiation and growth in austenitic stainless steels by laser peening without protective coating. *Mater. Sci. Eng. A*, **417**, 334–340.

10 Ben Fredj, N., Ben Nasr, M., Ben Rhouma, A., Braham, C. and Sidhom, H. (2004) Fatigue life improvements of the AISI 304 stainless steel ground surfaces by wire brushing. *J. Mater. Eng. Perform.*, **13**, 564–574.

11 Sidhom, N., Sidhom, H., Braham, C. and Lédion, J. (2011) Effects of brushing and shot-peening residual stresses on the fatigue resistance of machined metal surfaces: experimental and predicting approaches. *Mater. Sci. Forum.*, **681**, 290–295.

12 Makhlouf, K., Sidhom, N., Khlifi, A., Sidhom, H. and Braham, C. (2013) Low cycle fatigue life improvement of AISI 304 by initial and intermittent wire brush hammering. *Mater. Des.*, **52**, 1088–1098.

13 Zhang, P. and Lindemann, J. (2005) Effect of roller burnishing on the high cycle fatigue performance of the high-strength wrought magnesium alloy AZ80. *Scr. Mater.*, **52**, 1011–1015.

14 Smaga, M., Walther, F. and Eifler, D. (2008) Deformation-induced martensitic transformation in metastable austenitic steels. *Mater. Sci. Eng. A*, **483-484**, 394–397.

15 NF EN 15305 Avril. (2009) Essais non-destructifs: méthode d'essai pour l'analyse des contraintes résiduelles par diffraction des rayons X. AFNOR. 2009.

16 Ben Moussa, N., Sidhom, H. and Braham, C. (2012) Numerical and experimental analysis of residual stress and plastic strain distributions in machined stainless steel. *Int. J. Mech. Sci.*, **64**, 82–93.

17 Lu, J., Flavenot, J. F. and Turbat, A. (1988) Prediction of residual stress relaxation during fatigue. ASTM STP 993 (Editor by L. Mordfin), American Society for Testing and Materials, Philadelphia, pp. 75–90.

18 Capello, E., Davoli, P., Filippini, M. and Foletti, S. (2004) Relaxation of residual stresses induced by turning and shot peening of steels. *J. Strain Anal. Eng. Des.*, **39**, 285–290.

19 Torres, M. A. S. and Voorward, H. J. S. (2002) An evaluation of shot peening, residual stress and stress relaxation of the fatigue life of AISI 4340 steel. *Int. J. Fatigue*, **24**, 877–886.

20 Laamouri, A., Sidhom, H. and Braham, C. (2013) Evaluation of residual stress relaxation and its effect on fatigue strength of AISI 316L stainless steel ground surfaces: experimental and numerical approaches. *Int. J. Fatigue*, **48**, 109–121.

21 Ghanem, F., Ben Fredj, N., Sidhom, H. and Braham, C. (2011) Effects of finishing processes on the fatigue life improvements of electro-machined surfaces of tool steel. *Int. J. Adv. Manuf. Technol.*, **52**, 583–595.

22 Sidhom, N., Laamouri, A., Fathallah, R., Braham, C. and Lieurade, H. P. (2005) Fatigue strength improvement of 5083H11 Al-alloy T-welded joints by shot peening: experimental characterization and predictive approach. *Int. J. Fatigue*, **27**, 729–745.

23 Fathallah, R., Sidhom, H., Braham, C. and Castex, L. (2003) Effect of surface properties on high cycle fatigue behaviour of shot peened ductile steel. *Mater. Sci. Technol.*, **19**, 1050–1056.

24 Sidhom, N., Braham, C. and Lieurade, H. P. (2007) Fatigue life evaluation of shot peened al-alloys 5083H11T-welded joints by experimental and numerical approaches. *Weld. World*, **51**, 50–57.

25 Pippan, R., Zelger, C., Gach, E., Bichler, C. and Weinhandl, H. (2011) On the mechanism of fatigue crack propagation in ductile metallic materials. *FFEMS*, **34**, 1–16.